

# The Role of the Exciplex State in Photoinduced Electron Transfer of Phytochlorin–[60]Fullerene Dyads

Visa Vehmanen,<sup>\*,†</sup> Nikolai V. Tkachenko,<sup>†</sup> Alexander Efimov,<sup>†</sup> Pia Damlin,<sup>‡</sup> Ari Ivaska,<sup>‡</sup> and Helge Lemmetyinen<sup>†</sup>

*Institute of Materials Chemistry, Tampere University of Technology, P.O. Box 541, FIN-33101 Tampere, Finland, and Process Chemistry Group c/o Laboratory of Analytical Chemistry, Åbo Akademi University, FIN-20500 Turku-Åbo, Finland*

*Received: May 3, 2002; In Final Form: July 10, 2002*

The photoinduced electron transfer (ET) in five structurally different phytochlorin–fullerene dyads was studied in polar and nonpolar solvents using femtosecond fluorescence up-conversion and pump–probe transient-absorption techniques. Small changes in the structures of the dyads result in considerable changes in the ET properties and allow the determination of reorganization energies of the photoinduced reactions and electronic couplings between the initial and final states. After the excitation of the phytochlorin moiety to the second excited singlet state, the dyads relax rapidly to the first excited singlet state of phytochlorin. The first excited singlet state of phytochlorin is in equilibrium with an intramolecular exciplex state. In polar benzonitrile, the exciplex undergoes an electron transfer, and a complete-charge-separated (CCS) state is formed with a quantum yield close to unity. In contrast to the previously studied phytochlorin–fullerene dyads, the dyads in the present study form the CCS state also in nonpolar toluene with a yield influenced by minor changes in the molecular structure. The new dyads have a weaker phytochlorin–fullerene interaction due to longer separation distances between the two moieties. Therefore, the energies of the exciplex states are increased, and thus, their formation rates are reduced. In addition, the rates and yields of the complete charge separations are increased both in polar and nonpolar solvents. In benzonitrile, the reorganization energies for the transitions from the exciplex to the CCS and from the CCS to the ground state are 0.38 and 1.05 eV, respectively. The electronic couplings between the corresponding initial and final states of the two transitions mentioned above are 22 and 15 cm<sup>-1</sup>.

## Introduction

Undoubtedly, one of the most important chemical reactions in nature is the conversion of sunlight to chemical potential via photoinduced electron transfer (ET) in the photosynthetic reaction center. The process of photosynthesis has been widely studied not only for the sake of curiosity but also because of potentially important applications. In addition to an obvious objective of solar energy conversion, it has been acknowledged that artificial reaction centers also have potential uses in molecular-scale optoelectronics, photonics, sensor design, and other areas of nanotechnology.

During the past decade, porphyrin–fullerene donor–acceptor (DA) dyads have been in the focus of intensive research as candidates for artificial reaction centers.<sup>1–9</sup> Although fullerenes have a low absorbance in the visible part of the spectrum, porphyrins have strong absorption bands in this wavelength region. The dyads have shown promising results in molecular device applications for efficient conversion of light to electrostatic energy,<sup>10,11</sup> and they are considered good model systems of natural photosynthesis.<sup>1,2,12</sup> However, the natural photosynthesis utilizes chlorophylls in the reaction center, where the primary charge separation takes place, and as antenna molecules.<sup>13</sup> As these harvest light with higher efficiency relative

to fully conjugated porphyrins, it is quite surprising that relatively few DA dyads have been synthesized where a chlorophyll-like donor, instead of porphyrin, has been linked with fullerene.<sup>14–25</sup> The photochemical properties of some chlorin–fullerene dyads have been recently characterized.<sup>15–17,20,21</sup> Chlorin–fullerene systems can undergo photoinduced ET in solutions<sup>15,16,20,21</sup> and in solid state.<sup>17,18,26</sup>

An emissive intramolecular exciplex state played a crucial role in the photoinduced ET of previously studied phytochlorin–fullerene dyads, **PaF** and **PbF** (Figure 1).<sup>15–17</sup> In solutions, the exciplex was formed simultaneously via two pathways: (1) About half of the excited molecules relaxed extremely fast (in less than 200 fs) from the second excited singlet state of the phytochlorin moiety to the exciplex state.<sup>15</sup> (2) The rest of the excited molecules relaxed to the first excited singlet state of phytochlorin via an internal conversion. Then, an energy transfer from phytochlorin to fullerene took place followed by a relaxation to the exciplex state. Therefore, it was concluded that the energy of the exciplex is less than that of the fullerene singlet excited state. In nonpolar solvents, the exciplex states of **PaF** and **PbF** decayed directly to the ground state. In polar benzonitrile, a complete charge separated (CCS) state was formed from the **PaF** exciplex,<sup>15</sup> whereas the **PbF** exciplex decayed directly to the ground state.<sup>16</sup>

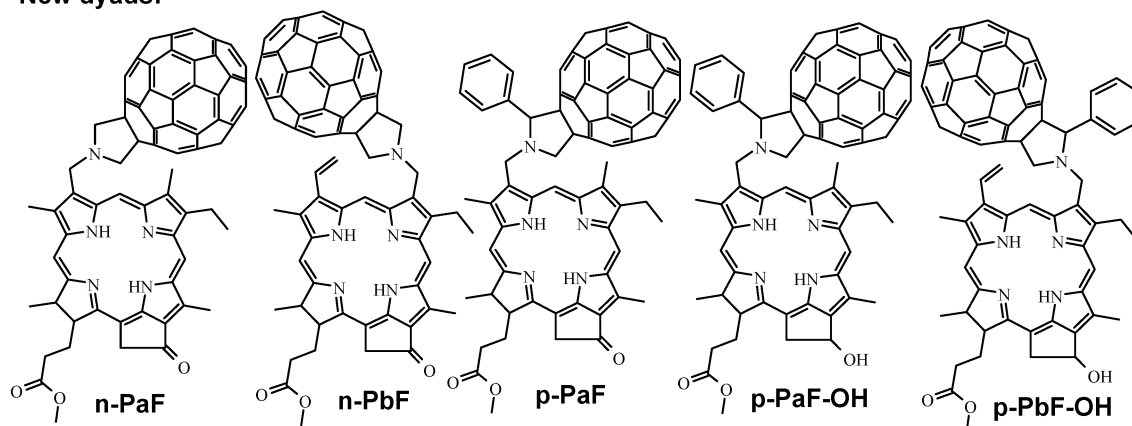
In solid Langmuir–Blodgett (LB) films, after the exciplex formation, a vectorial photoinduced ET took place for **PaF**.<sup>17</sup> However, the fraction of **PaF** molecules capable of electron

\* To whom correspondence should be addressed. E-mail: visa.vehmanen@tut.fi. Fax: +358 3 365 2108. Phone: +358 3 365 3627.

<sup>†</sup> Tampere University of Technology.

<sup>‡</sup> Åbo Akademi University.

## New dyads:



## Reference compounds:

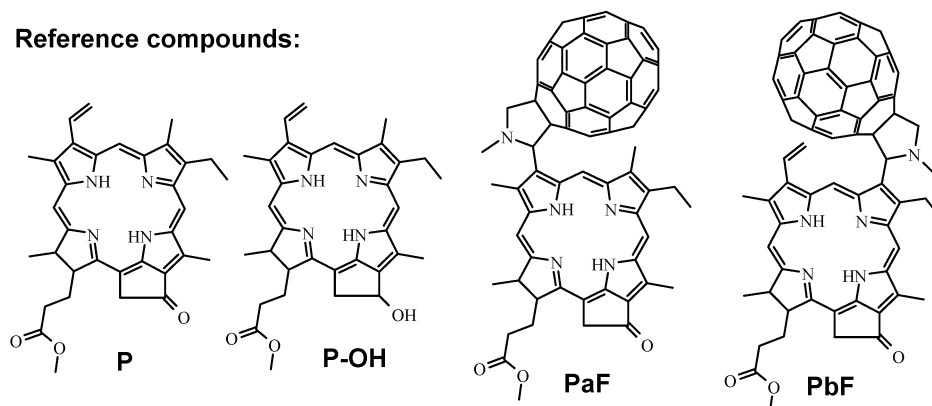


**Figure 1.** Molecular structures of the studied and reference compounds.

transfer was only 0.2%. In LB films, the **PaF** molecules were incorporated into a nonpolar matrix, whereas it was known that the CCS state is not formed in nonpolar solvents.<sup>15</sup> It is obvious that the ET properties of the **PaF** and **PbF** dyads left a lot of room for improvement especially in the nonpolar environment.

It may be that the energy of the exciplex is too low for the CCS state to be formed efficiently in **PaF** and **PbF**. Therefore, if the energy of the exciplex state is increased or the energy of the CCS state is decreased, a complete charge separation can take place. To achieve these changes in the intermediate state energies, a series of five new phytochlorin–fullerene dyads (Figure 1) have been synthesized.<sup>19</sup>

The new dyads have a longer bridge between the phytochlorin and the fullerene relative to **PaF** and **PbF**.<sup>15,16</sup> This should reduce the electronic coupling between the phytochlorin and fullerene moieties and thus increase the energy of the exciplex state. In addition, two of the new dyads, **p-PaF-OH** and **p-PbF-OH**, have a hydroxyl substituent at the position 13<sup>1</sup> of the phytochlorin macrocycle instead of a keto group. The reduction of the keto group to the less electron withdrawing hydroxyl group should lower the oxidation potential of the phytochlorin and, therefore, decrease the energy of the CCS state.

In the dyads used in this study, the first excited singlet state of phytochlorin is in equilibrium with an exciplex state, indicating that the exciplex state energy is increased relative to **PaF** and **PbF**. In polar benzonitrile, the exciplex state undergoes an electron transfer, and a CCS state is formed with a quantum yield close to unity, whereas in **PaF**, the yield was clearly less. It is possible to determine the reorganization energies of the ET reactions for structurally very similar dyads, **p-PaF** and **p-PaF-OH**. The reorganization energies allow the calculation

of the electronic couplings between the initial and final states of the corresponding reactions. In contrast to **PaF** and **PbF**, the dyads presented in this study form the CCS state also in nonpolar toluene with efficiency depending on the small differences in the molecular structure. The formation of the CCS state in the nonpolar environment is important from the point of possible optoelectronic applications of these molecules.

## Results

**Steady-State Spectroscopy.** The structures of the studied dyads (**n-PaF**, **n-PbF**, **p-PaF**, **p-PaF-OH**, and **p-PbF-OH**) and the phytochlorin reference compounds (**P** and **P-OH**) are shown in Figure 1. The absorption spectra of two phytochlorin–fullerene dyads (**n-PaF** and **n-PbF**) and the reference compounds, 3<sup>1</sup>,3<sup>2</sup>-didehydrophytochlorin (**P**) and [60]fullerene (**C<sub>60</sub>**), in toluene are shown in Figure 2a. Figure 2b shows absorption spectra of 3<sup>1</sup>,3<sup>2</sup>-didehydro-13<sup>1</sup>-desoxy-13<sup>1</sup>-hydroxyphytochlorin (**P-OH**), two phytochlorin–fullerene dyads (**p-PaF** and **p-PaF-OH**), and [60]fullerene (**C<sub>60</sub>**) in toluene. The hydroxyl group of **p-PaF-OH** (position 13<sup>1</sup> of the phytochlorin macrocycle) shifts the absorption of the Soret band and the first *Q*-band of the phytochlorin moiety to the blue by about 10 nm relative to those of **p-PaF**. Thus, the second and first excited singlet states of the phytochlorin moiety are higher in energy for **p-PaF-OH** and **p-PbF-OH** than for **n-PaF**, **n-PbF**, and **p-PaF**. The absorption spectrum of the **p-PbF-OH** dyad is presented in Figure S1 (see the Supporting Information).

The fluorescence of the DA compounds originates mainly from the phytochlorin moiety. The fluorescence spectra of the **n-PbF** and **p-PaF** dyads with the phytochlorin reference, **P**, are shown in Figure 3. As compared with the corresponding

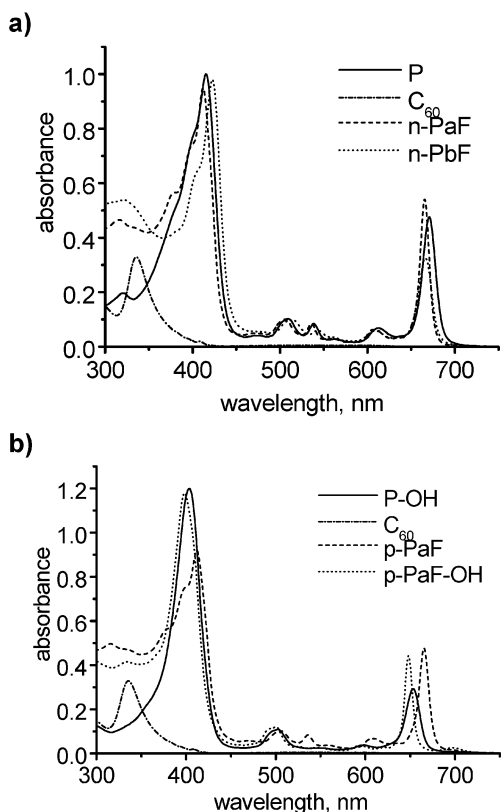


**Figure 2.** Absorption spectra of (a) **P**, **C<sub>60</sub>**, **n-PaF**, and **n-PbF** and (b) **P-OH**, **C<sub>60</sub>**, **p-PaF**, and **p-PaF-OH** in toluene. Sample concentrations are 10  $\mu\text{M}$ .

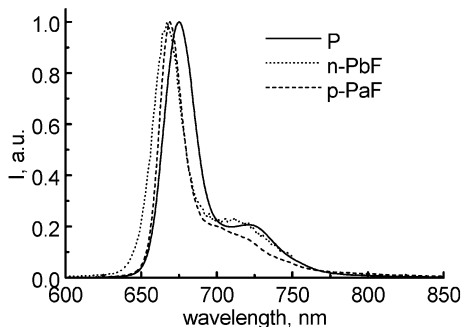


**Figure 3.** Normalized fluorescence emission spectra of **P**, **n-PbF**, and **p-PaF** in toluene.

phytychlorin (**P** or **P-OH**), the relative fluorescence intensities of the dyads **n-PaF**, **n-PbF**, **p-PaF**, **p-PaF-OH**, and **p-PbF-OH** are 1/400, 1/70, 1/50, 1/100, and 1/100, respectively, indicating that the emission of the phytychlorin first excited singlet state in the dyads is strongly quenched.

**Time-Resolved Emission Decays.** In the fluorescence up-conversion and pump-probe transient-absorption experiments, the used excitation wavelengths were between 400 and 420 nm, where the absorption of the phytychlorin moiety is much stronger than that of the fullerene. Therefore, the second excited singlet state of the phytychlorin,  $P^{25}C$ , was formed right after the 50 fs excitation pulse. The excitation to the  $P^{25}C$  state was followed by an internal conversion where the phytychlorin moiety of the dyads relaxed rapidly to its first excited singlet state,  $P^{15}C$ . The internal conversion was not resolved in time, and the first spectroscopically observed state was  $P^{15}C$ .

The population of the  $P^{15}C$  state in any of the dyads can be monitored by measuring the fluorescence decay profile at the wavelength of maximum phytychlorin emission, e.g., 670 nm

**TABLE 1: Fitted Lifetimes and Their Relative Amplitudes of the Fluorescence Decay Monitored at the Wavelength of the Maximum Emission of the Phytychlorin Moiety of the Dyad<sup>a</sup>**

compound	$\tau_1$ , ps (rel. amp.)	$\tau_2$ , ps (rel. amp.)	$\tau_3$ , ps (rel. amp.)	$a_1/a_2$
Benzonitrile				
n-PaF	2.5 (28%)	7.5 (64%)	70 (8%)	0.43
n-PbF	1.3 (34%)	10 (55%)	80 (12%)	0.60
p-PaF	2.4 (26%)	12 (69%)	100 (5%)	0.38
p-PaF-OH	1.5 (92%)	15 (8%)		11.0
p-PbF-OH	1.3 (52%)	6.5 (35%)	70 (14%)	1.49
Toluene				
n-PaF	5.3 (32%)	21 (68%)		0.47
n-PbF	3.7 (36%)	20 (36%)	100 (28%)	0.99
p-PaF	5.0 (21%)	26 (75%)	1000 (4%)	0.28
p-PaF-OH	1.5 (90%)	27 (10%)		8.82
p-PbF-OH	1.1 (55%)	7.2 (33%)	50 (12%)	1.64

<sup>a</sup> Ratio of the first two amplitudes is given in the last column.

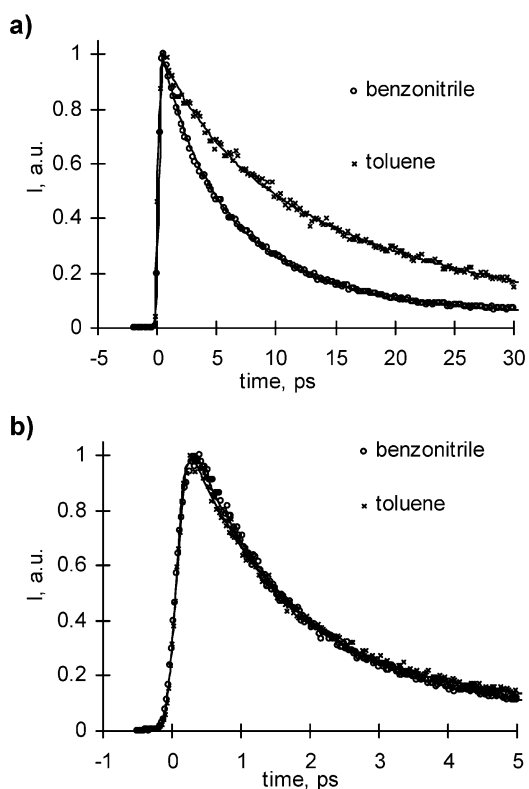


**Figure 4.** Fluorescence decays of the dyads in benzonitrile and toluene: (a) **n-PaF** monitored at 670 nm and (b) **p-PaF-OH** monitored at 655 nm. Solid lines represent the fittings.

for **n-PaF** in toluene. Kinetics of the fluorescence decays of  $P^{15}C$  required at least biexponential fitting. When a three-exponential fitting was needed, the relative amplitude of the longest-lived component was the smallest. The longest-lived component may be attributed to sample degradation under intense excitation light, which is required by the up-conversion technique. Therefore, in further discussion, the fluorescence decay of the  $P^{15}C$  state is considered biexponential for all of the dyads. The fluorescence lifetimes and their relative amplitudes are collected in Table 1.

As an example, the decays of  $P^{15}C$  emissions at 670 nm are shown in Figure 4a for **n-PaF** in benzonitrile and in toluene. In toluene, the decay is two-exponential, whereas in benzonitrile, a three-exponential fitting is required. The lifetimes for **n-PaF** are 5.3 (32% relative amplitude) and 21 ps (68%) in toluene but 2.5 (28%), 7.5 (64%), and 70 ps (8%) in benzonitrile.

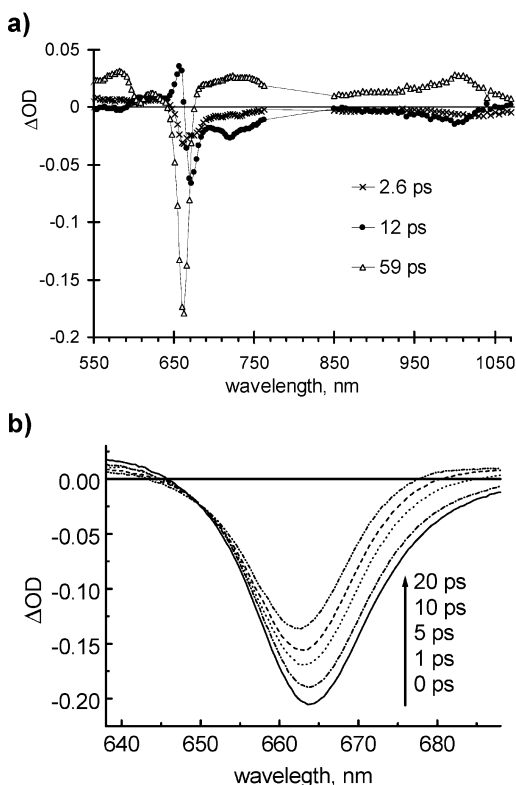


**Figure 5.** (a) Absorption component spectra of the transients for **n-PaF** in benzonitrile. Lifetimes of the components are indicated. (b) Transient-absorption spectra at different delay times for **n-PaF** in benzonitrile.

For **n-PaF**, **n-PbF**, and **p-PaF**, the decays were faster in benzonitrile than in toluene. The hydroxyl dyads, **p-PaF-OH** and **p-PbF-OH**, decayed faster than the keto dyads, and the relative amplitudes of their first components were higher. The decays in benzonitrile and toluene were almost identical for **p-PaF-OH** (Figure 4b) and for **p-PbF-OH**.

**Transient-Absorption Measurements.** Transient-absorption spectra of the dyads were recorded using the pump-probe technique in two wavelength domains. The *Q*-band region (550–770 nm) gives information about the photoprocesses of the phytychlorin part, whereas the signal in the NIR (850–1070 nm) is mainly due to the transients of the fullerene moiety. Multiexponential global fittings were applied to transient-absorption decay curves at different wavelengths.<sup>15</sup>

Both in benzonitrile and in toluene, three-exponential fittings gave reasonable results for all of the dyads. The addition of a fourth exponential to the fitting did not improve the statistical reliability in terms of the mean-square deviation, and a fitting with two exponentials caused significantly worse results. Hence, three intermediate states are time-resolved in the decay of all of the dyads both in benzonitrile and in toluene. Because the results of the transient-absorption measurements are, in principle, very alike for all of the dyads, the component spectra in benzonitrile and in toluene are presented and discussed in detail only for **n-PaF** (Figures 5a and 6a, respectively). The lifetimes of the components of all of the dyads in the transient-absorption decay are collected in Table 2.

The dyads were excited to the second excited singlet state of phytychlorin,  $P^{2S}$ . The internal conversion ( $P^{2S} \rightarrow P^{1S}$ ) is very fast and not resolved in time. Therefore, the shortest-lived component in transient absorption of **n-PaF** in benzonitrile (Figure 5a) can be attributed to the  $P^{1S}$  state. The longest-lived (59 ps) component has still a strongly bleached *Q*-band at 660 nm, indicating that the phytychlorin moiety of the excited

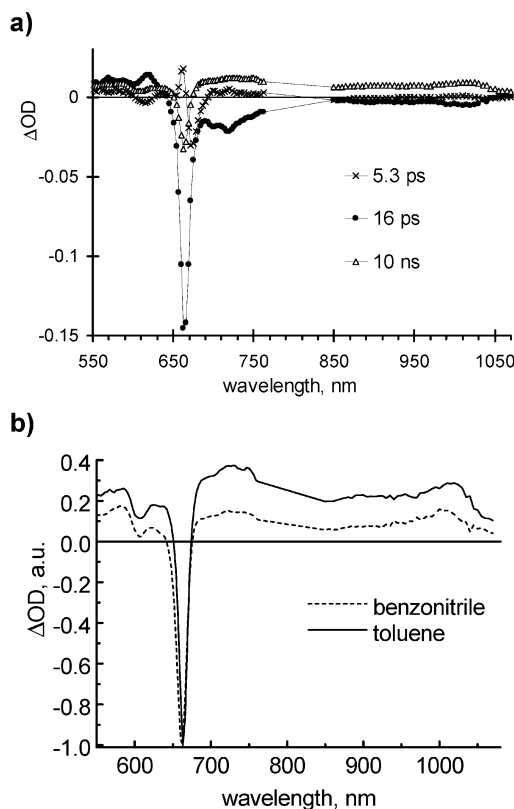


**Figure 6.** (a) Absorption component spectra of the transients for **n-PaF** in toluene. Lifetimes of the components are indicated. (b) The longest-lived components for **n-PaF** in benzonitrile and toluene. Maximum *Q*-band bleaching is normalized to  $-1$ .

**TABLE 2: Fitted Lifetimes of the Transient-Absorption Decays**

compound	$\tau_1$ , ps	$\tau_2$ , ps	$\tau_3$ , ps
Benzonitrile			
n-PaF	2.6	12	59
n-PbF	1.8	13	100
p-PaF	4	14	72
p-PaF-OH	1.2	11	27
p-PbF-OH	1.4	7	49
Toluene			
n-PaF	5.3	16	10000
n-PbF	5.5	25	3000
p-PaF	5.0	23	4000
p-PaF-OH	1.8	21	3000
p-PbF-OH	2.0	93	4000

dyad is not in its ground state. The component also has a pronounced band at 1010 nm, which is attributed to the fullerene anion.<sup>12,27–30</sup> Thus, the longest-lived (59 ps) component can be identified as the CCS state.

The lifetimes of the shortest-lived (2.6 ps) and the middle-lived component (12 ps) correlate reasonably well with the lifetimes of the biexponential decay of the  $P^{1S}$  emission, 2.5 and 7.5 ps. Several conformers of the dyads could be present simultaneously because of the flexible bridge between the phytychlorin and fullerene moieties. Thus, the biexponential decay of the emission could be explained by the decays of the  $P^{1S}$  states of two conformers to the CCS states. Then, the 2.6 and 12 ps components would be expected to have the same shape, and a two exponential decay of two different CCS states should be observed. However, the shape of the 12 ps components is clearly different, and only a monoexponential decay of the absorption of the CCS state was observed for all



of the dyads in benzonitrile. Therefore, the existence of more than one conformer is not needed to explain the observed results. The biexponential decay of the  $P^{1S}C$  emission can be explained by an equilibrium between the  $P^{1S}C$  state and some other state. Thus, the middle-lived component in the transient absorption is attributed to the state in equilibrium with  $P^{1S}C$ .

The energy transfer from phytochlorin to fullerene was an efficient channel for quenching of the  $P^{1S}C$  state of **PaF** (Figure 1).<sup>15</sup> In the present study, however, no evidence of intramolecular energy transfer was obtained in benzonitrile. Figure 5b shows the  $Q$ -band region of the transient-absorption spectra measured for the **n-PaF** dyad in benzonitrile at different delay times after excitation. The  $Q$  band remains strongly bleached for at least 20 ps after the excitation. This indicates that the middle-lived component (12 ps) must be attributed to a state, where the phytochlorin moiety is not in its ground state. Therefore, it cannot be attributed to the first excited singlet state of fullerene. If this were the case, the  $Q$  band should recover after the decay of the  $P^{1S}C$  state as it was observed in the case of **PaF**,<sup>15</sup> where an energy transfer from phytochlorin to fullerene took place.

The middle-lived component is attributed to an exciplex,  $(PC)^*$ , which has been observed to precede the CCS state in photoinduced ET of the **PaF** dyad.<sup>15,16</sup> In addition, it has been recently reported that the porphyrin first excited singlet state can be in equilibrium with the exciplex of porphyrin–fullerene dyads.<sup>31</sup>

Three transient-absorption components were observed also in a toluene solution of **n-PaF** (Figure 6a). The lifetime of the longest-lived component (10 ns) was too long to be determined accurately by the instrument used, where the longest available delay time is 1 ns. The first step of the photoinduced process is the same as in benzonitrile, as indicated by the biexponential decay of  $P^{1S}C$  emission and strong bleaching of the  $Q$ -band absorption during the first 20 ps after the excitation. Therefore, the shortest-lived and the middle-lived components in the transient absorption are attributed to the  $P^{1S}C$  and  $(PC)^*$  states, respectively.

The longest-lived (10 ns) component in toluene has a bleached  $Q$  band and a characteristic fullerene anion absorption band<sup>12,27–30</sup> at around 1010 nm implying the presence of a CCS state. Nevertheless, there is only about  $1/4$  of the initial bleaching of the  $Q$  band left (Figure 6a) indicating that about  $3/4$  of the dyads have the phytochlorin moiety in its ground state. Figure 6b shows that the longest-lived component in toluene cannot be attributed to the CCS state alone, since it has much stronger absorption in the wavelength range of 700–1000 nm relative to the component in benzonitrile, which represents the differential transient spectrum of the CCS state. The stronger absorption in toluene is explained by the formation of both the CCS state and the first excited singlet state of fullerene,  $PC^{1S}$ , after the decay of the exciplex. The first excited singlet state of fullerene has a broad structureless absorption in the wavelength range of 600–1000 nm.<sup>32,33</sup> However, if both the CCS and the  $PC^{1S}$  states are formed, a four-exponential transient-absorption decay should be observed instead of the three-exponential decay. The  $PC^{1S}$  state should have a 1.4 ns lifetime due to the intersystem crossing to the triplet state,  $PC^{1T}$ ,<sup>34–36</sup> which is too long a lifetime to be determined accurately by the used pump–probe instrument. Therefore, the 10 ns component could be a sum of two long-lived components, which are observed as one component because of the limited time scale of the instrument ( $\sim 1$  ns). In principle,  $PC^{1S}$  could also decay to the CCS state

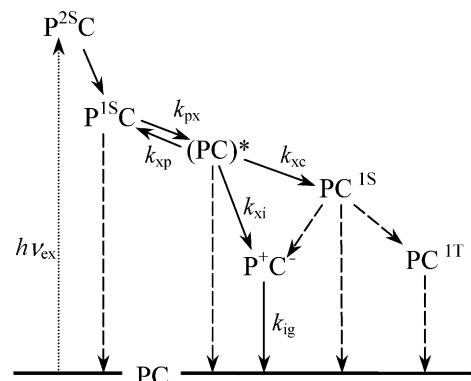


**Figure 7.** Proposed kinetic scheme for the photoinduced reactions of the studied compounds. Experimentally observed steps are indicated with the solid arrows and the supposed reactions with the dashed arrows.

but there was no experimental evidence indicating such transition.

## Discussion

**Scheme and Intrinsic Rates.** The results of the time-resolved measurements of the studied dyads in benzonitrile and toluene can be summarized to a common scheme, which is presented in Figure 7. The different states are the ground state (g), the excited singlet states of phytochlorin (p) and fullerene (c), the exciplex (x), and the complete charge-separated state (i). For the dyads in benzonitrile, no evidence of the first excited singlet state of fullerene was obtained. Therefore, the rate  $k_{xc}$  is negligible, and the time profile of the phytochlorin emission is determined by three intrinsic rate constants:  $k_{px}$ ,  $k_{xp}$ , and  $k_{xi}$  (Figure 7), where the two letters in the subscripts of the rate constant symbols denote the initial and final states of the transitions, respectively. The experimentally obtained parameters are the two emission decay time constants,  $\tau_1$  and  $\tau_2$ , and the ratio of the preexponential factors,  $r = a_1/a_2$ . If the initially populated state is the first excited singlet state of the phytochlorin, i.e.,  $[P^{1S}C] = 1$  and  $[(PC)^*] = 0$  at  $t = 0$ , the intrinsic rate constants can be calculated. As shown in the Supporting Information, the intrinsic rate constants can be expressed using experimentally available parameters as follows:

$$k_{px} = \frac{r\lambda_1 + \lambda_2}{-r - 1}$$

$$k_{xi} = \frac{\lambda_1\lambda_2}{k_{px}}$$

$$k_{xp} = -\lambda_1 - \lambda_2 - k_{px} - k_{xi} \quad (1)$$

where  $\lambda_1 = -1/\tau_1$  and  $\lambda_2 = -1/\tau_2$ .

For the dyads in toluene, the time profile of the phytochlorin emission is determined by four intrinsic rate constants:  $k_{px}$ ,  $k_{xp}$ ,  $k_{xi}$ , and  $k_{xc}$ . If the sum of the rates  $k_{xi}$  and  $k_{xc}$  is denoted by  $k_{sum}$ , a similar analysis for the rates in toluene can be done as in benzonitrile. Then, the rates  $k_{xi}$  and  $k_{xc}$  can be calculated, because the ratio  $k_{xi}/k_{xc}$  is available experimentally (see “Quantum yield of the CCS state in toluene”).

The rate of the charge recombination,  $k_{ig}$ , is determined from the lifetime of the longest-lived component in the transient-absorption decay,  $k_{ig} = 1/\tau_3$ . For the dyads in toluene, the lifetimes of the longest-lived components were clearly longer than 1 ns. Therefore,  $k_{ig} < 1 \text{ ns}^{-1}$  in toluene. The calculated rate constants in benzonitrile and toluene are presented in Table 3.

**TABLE 3: Reaction Rate Constants and Free Energies Calculated According to the Scheme Presented in Figure 7<sup>a</sup>**

compd	$k_{px}$ , $10^9 \text{ s}^{-1}$	$k_{xp}$ , $10^9 \text{ s}^{-1}$	$k_{xi}$ , $10^9 \text{ s}^{-1}$	$k_{xc}$ , $10^9 \text{ s}^{-1}$	$k_{ig}$ , $10^9 \text{ s}^{-1}$	$-\Delta G_{px}$ , eV
Benzonitrile						
n-PaF	210	70	250	0	17	0.029
n-PbF	340	290	210	0	10	0.004
p-PaF	170	130	200	0	14	0.008
p-PaF-OH	610	44	70	0	40	0.068
p-PbF-OH	540	190	230	0	20	0.028
Toluene						
n-PaF	92	47	29	68	<1	0.018
n-PbF	160	77	25	60	<1	0.019
p-PaF	81	49	48	72	<1	0.013
p-PaF-OH	600	60	33	8	<1	0.060
p-PbF-OH	630	230	170	40	<1	0.026

<sup>a</sup> The subscripts refer to the initial and final states of the transition, respectively: p = P<sup>1S</sup>C, x = (PC)\*, c = PC<sup>1S</sup>, i = P<sup>+</sup>C<sup>-</sup>, g = PC.

**Energies of the Intermediate States.** The energies of the P<sup>1S</sup>C states (1.92–1.86 eV) of the dyads relative to the ground state are known from the steady-state absorption and emission measurements. The energy of the first excited singlet state of fullerene, PC<sup>1S</sup>, is 1.74 eV.<sup>2</sup> The calculated rate constants for the equilibrium (P<sup>1S</sup>C ↔ (PC)\*) allow the estimation of the energy difference between the two states:  $\Delta E = k_B T \ln(k_{px}/k_{xp})$ . The results are presented in Table 3. The calculated energy differences between the states in the equilibrium (0.004–0.068 eV depending on the dyad and the solvent) are clearly smaller than the energy differences between the P<sup>1S</sup>C and PC<sup>1S</sup> states (0.12–0.18 eV), which is another indication that the state in equilibrium with the P<sup>1S</sup>C state is not PC<sup>1S</sup>. Because the energy of the P<sup>1S</sup>C is known, the corresponding energy of the exciplex can be calculated.

To estimate the energies of charge-separated states formed after the excitation, the first oxidation potential of the phytychlorin moiety and the first reduction potential of the fullerene are required. These were determined by performing cyclic voltammetry experiments of the dyads and the reference compounds in benzonitrile solution. The **n-PaF** dyad was found to exhibit a first reversible oxidation potential of +0.86 V (vs Ag/AgCl), which is ascribed to the phytychlorin moiety based on the results of reference phytychlorin, **P** (+0.84 V). The first reduction potential of –0.55 V is due to formation of the fullerene radical anion based on the measurement of fullerene reference (–0.57 V). For the hydroxyl dyad, **p-PaF-OH**, the first oxidation potential was considerably lower (+0.68 V), as was expected based on the result of reference phytychlorin, **P-OH** (+0.64 V). The values of the intermediate state energies are listed in Table 4.

#### Transient-Absorption Spectra of the Intermediate States.

On the basis of the proposed kinetic scheme (Figure 7) and the experimental results, the differential absorption spectra of the intermediate states can be calculated. The differential transient absorbance at wavelength  $\lambda$  and time  $t$  is given by  $\Delta A(\lambda, t) = \sum a_i(\lambda) \exp(-t/\tau_i)$  where  $a_i(\lambda)$  and  $\tau_i$  are the amplitudes and lifetimes, respectively, of the components in the decay-associated spectra (DAS). The spectra of the P<sup>1S</sup>C and CCS states are easily obtained from the measured transient-absorption component spectra for **n-PaF** in benzonitrile. At  $t = 0$ , only the first transient state is populated, and its spectrum is given by  $\sum a_i(\lambda)$ . This is how the spectrum of P<sup>1S</sup>C for **n-PaF** was obtained (Figure 8). The longest-lived component corresponds to the transient absorption when only the last transient, the CCS state, is left.

**TABLE 4: Energies of the Intermediate States Relative to the Ground State**

compound	P <sup>1S</sup> C, eV	(PC)*, eV	PC <sup>1S</sup> , eV	P <sup>+</sup> C <sup>-</sup> , eV
Benzonitrile				
n-PaF	1.87	1.84	1.74	1.41
n-PbF	1.86	1.86	1.74	<i>a</i>
p-PaF	1.87	1.86	1.74	1.45
p-PaF-OH	1.92	1.85	1.74	1.26
p-PbF-OH	1.91	1.88	1.74	<i>a</i>
Toluene				
n-PaF	1.86	1.85	1.74	
n-PbF	1.86	1.84	1.74	
p-PaF	1.86	1.85	1.74	
p-PaF-OH	1.91	1.85	1.74	
p-PbF-OH	1.91	1.88	1.74	

<sup>a</sup> Value was not measured due to lack of substance.

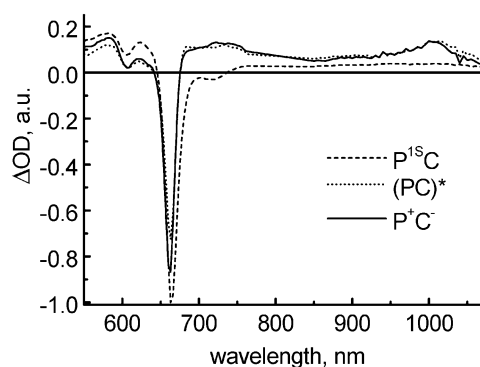


**Figure 8.** Normalized differential transient spectra of P<sup>1S</sup>C, (PC)\*, and P<sup>+</sup>C<sup>-</sup> states of **n-PaF** in benzonitrile. For the P<sup>1S</sup>C state, the maximum *Q*-band bleaching is normalized to –1, and the spectra of the (PC)\* and P<sup>+</sup>C<sup>-</sup> states are multiplied by the same normalization coefficient.

Because the kinetic scheme for the dyads contains an equilibrium between the P<sup>1S</sup>C and (PC)\* states, there is no time delay at which the transient-absorption spectrum would represent purely the absorption of the exciplex. An expression for calculating the spectrum of the exciplex is derived in SI. The results of the calculations are presented for **n-PaF** in benzonitrile in Figure 8.

The differential absorption spectrum of the P<sup>1S</sup>C state has a band between 550 and 650 nm, a bleached *Q* band, and a very weak absorption between 700 and 1050 nm. The bleached *Q* band in the calculated spectrum of the exciplex, (PC)\*, confirms that the phytychlorin moiety is not in its ground state. The absorption spectra of the exciplex and the CCS state are very alike, e.g. the exciplex has an absorption band at around 1010 nm. The close resemblance of the spectra, which is due to the partial charge-transfer character of the exciplex state, makes the detection of the exciplex difficult based on the transient-absorption measurements alone.

**Quantum Yield of the CCS State in Toluene.** On the basis of the spectra of the longest-lived states in benzonitrile and toluene, the quantum yield of the CCS state in toluene can be estimated. It is assumed that in benzonitrile all of the excited molecules undergo a complete charge transfer and form the CCS state. The normalized transient spectra of the longest-lived states are compared in Figure 9a. From the ratio of the *Q*-band bleaching in benzonitrile and toluene (lines 1 and 2 in Figure 9a), it is possible to determine the fraction of the molecules in toluene, where the phytychlorin moiety is not in its ground state. The quantum yield of CCS for **n-PaF** is 0.3, and the rest of the molecules convert to the PC<sup>1S</sup> state. Therefore, the ratio of the

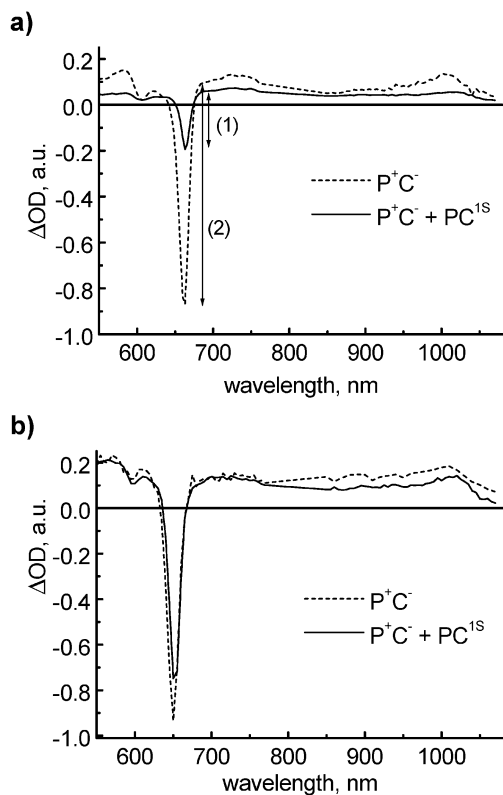


**Figure 9.** Normalized differential transient spectra of  $P^+C^-$  in benzonitrile (dashed line) and  $P^+C^- + PC^{1S}$  in toluene (solid line) for (a) **n-PaF** and (b) **p-PbF-OH**. The maximum  $Q$ -band bleachings of the spectra of the  $P^{1S}C$  states (not shown in the Figure) were normalized to  $-1$ , and the spectra of the  $P^+C^-$  states were multiplied by the same normalization coefficient.

**TABLE 5: Quantum Yield ( $\Phi_{CCS}$ ) of the CCS State in Benzonitrile and Toluene**

compound	$\Phi_{CCS}$ benzonitrile	$\Phi_{CCS}$ toluene
n-PaF	$\sim 1$	0.3
n-PbF	$\sim 1$	0.3
p-PaF	$\sim 1$	0.4
p-PaF-OH	$\sim 1$	0.8
p-PbF-OH	$\sim 1$	0.8

rates  $k_{xi}/k_{xc} = 0.3/0.7 = 0.43$ , which is used to calculate the rates  $k_{xi}$  and  $k_{xc}$  in toluene.

In toluene, the quantum yields of the CCS state formation of the hydroxyl dyads (**p-PaF-OH** and **p-PbF-OH**) are clearly higher than the yields of the keto dyads (Table 5). The quantum yields are obtained from the normalized spectra of the longest-lived states in benzonitrile and toluene (Figure 9b).

**Comparison of Electron-Transfer Properties.** The structural differences of the five studied dyads (**n-PaF**, **n-PbF**, **p-PaF**, **p-PaF-OH**, and **p-PbF-OH**) are (1) the presence of a keto or a hydroxyl group at the position 13<sup>1</sup> of the phytychlorin macrocycle, (2) the position to which the pyrrolidine bridge-fullerene is linked relative to the phytychlorin macrocycle and the presence of a vinyl group at the position 3, and (3) the presence or absence of a phenyl group at the position 2' in the pyrrolidine ring.

Most pronounced differences in the photoprocesses are related to the reduction of the keto group to the hydroxyl group at the position 13<sup>1</sup>. The effect of this change can be observed by comparing otherwise similar dyads, **p-PaF** and **p-PaF-OH**. The reduction increases the energy of the  $P^{1S}C$  state in **p-PaF-OH** by 0.05 eV relative to **p-PaF**, which can be observed in

the absorption spectra (Figure 2b), and reduces the oxidation potential of the dyad and the energy of the CCS state by 0.19 V and 0.19 eV, respectively. The emission decay of **p-PaF-OH** is almost monoexponential indicating a larger energy difference between  $P^{1S}C$  and  $(PC)^*$ , and the formation rate of the exciplex is higher for **p-PaF-OH** in both solvents. The rate of the transition from the exciplex to the first excited singlet state of fullerene is almost 10 times lower for **p-PaF-OH** than for **p-PaF** in toluene. The quantum yield of the CCS state in toluene is 0.8 for **p-PaF-OH** and only 0.4 for **p-PaF**. The charge recombination rate is higher for **p-PaF-OH** in benzonitrile.

It seems that the effect of the hydroxyl group is similar to the insertion of a central metal, e.g., Zn, to the phytychlorin macrocycle. In phytychlorin-fullerene dyads, the presence of the central zinc atom, which reduces the oxidation potential of the phytychlorin macrocycle,<sup>20</sup> increases the rates of the CCS formation and the charge recombination relative to the free-base analogues.<sup>15</sup>

For the hydroxyl dyads, **p-PaF-OH** and **p-PbF-OH**, the exciplex formation rate seems to be independent of solvent, whereas for the keto dyads, **n-PaF**, **n-PbF**, and **p-PaF**, the formation rate is clearly lower in toluene. The formation rate of the CCS state, however, is higher for all the dyads in benzonitrile than in toluene.

The influence of the attachment position of the pyrrolidine bridge-fullerene and the presence of a vinyl group at the position 3 can be seen by comparing otherwise similar dyad pairs, **n-PaF** and **n-PbF** or **p-PaF-OH** and **p-PbF-OH**. The formation rate of the CCS state is about 3 times higher for **p-PbF-OH** than for **p-PaF-OH** in benzonitrile. The CCS formation and energy transfer ( $(PC)^* \rightarrow PC^{1S}$ ) rates are about 5 times higher for **p-PbF-OH** than for **p-PaF-OH** in toluene. For **n-PaF** and **n-PbF**, the differences in the CCS formation and energy transfer rates are not reliable. The quantum yields of the CCS states in toluene are the same for the *a* and *b* derivatives of the dyads, whereas the charge recombination rates are about two times lower for the *b* derivatives in benzonitrile.

The effect of the presence or absence of the phenyl group at the position 2' in the pyrrolidine ring can be seen by comparing the two otherwise alike dyads, **n-PaF** and **p-PaF**. There are relatively small differences between the rates of **n-PaF** and **p-PaF**, but in toluene, the CCS state is formed with higher quantum yield for **p-PaF** (0.4 vs 0.3).

On the basis of the transient-absorption measurements in benzonitrile, the dyads are assumed to form the CCS state with a quantum yield close to unity. The lifetime of the CCS state in toluene is more than 1 order of magnitude longer than in benzonitrile. In toluene, **p-PaF-OH** and **p-PbF-OH** form the CCS state with quantum yield of 0.8, but the CCS formation rate for **p-PbF-OH** is about 5 times higher than for **p-PaF-OH**.

**Reorganization Energy and Electronic Coupling.** For a diabatic reaction, the ET rate is given by the equation<sup>37</sup>

$$k = \frac{2\pi^{3/2}}{h} \frac{V^2}{(\lambda k_B T)^{1/2}} \exp\left(-\frac{(\Delta G^0 + \lambda)^2}{4\lambda k_B T}\right) \quad (2)$$

where  $V$  is the electronic coupling matrix element,  $\lambda$  is the reorganization energy, and  $\Delta G^0$  is the reaction free energy. For the studied dyads, there are two unknown parameters in eq 2: the electronic coupling matrix element,  $V$ , and the reorganization energy,  $\lambda$ . The **p-PaF** and **p-PaF-OH** dyads have very similar structures, with the only difference being the presence of either



a keto or a hydroxyl group at the position 13<sup>1</sup> of the phytychlorin macrocycle. Therefore, it is reasonable to assume that the reorganization energies and the electronic couplings of the ET reactions are the same. Thus, the ratio of the ET rate constants of **p-PaF** and **p-PaF-OH** does not depend on the electronic coupling:

$$\frac{k_{\text{p-PaF}}}{k_{\text{p-PaF-OH}}} = \exp\left(-\frac{(\Delta G_{\text{p-PaF}}^0 + \lambda)^2}{4\lambda k_{\text{B}}T} + \frac{(\Delta G_{\text{p-PaF-OH}}^0 + \lambda)^2}{4\lambda k_{\text{B}}T}\right) \quad (3)$$

Reorganization energy can be obtained from eq 3

$$\lambda = \frac{(\Delta G_{\text{p-PaF-OH}}^0)^2 - (\Delta G_{\text{p-PaF}}^0)^2}{2(2\alpha k_{\text{B}}T - \Delta G_{\text{p-PaF-OH}}^0 + \Delta G_{\text{p-PaF}}^0)} \quad (4)$$

where  $\alpha = \ln(k_{\text{p-PaF}}/k_{\text{p-PaF-OH}})$ . For the charge recombination reactions ( $\text{P}^+\text{C}^- \rightarrow \text{PC}$ ) in benzonitrile, the rate constants and the reaction free energies are  $k_{\text{p-PaF}} = 14 \times 10^9 \text{ s}^{-1}$ ,  $k_{\text{p-PaF-OH}} = 40 \times 10^9 \text{ s}^{-1}$ ,  $\Delta G_{\text{p-PaF}}^0 = -1.45 \text{ eV}$ , and  $\Delta G_{\text{p-PaF-OH}}^0 = -1.26 \text{ eV}$  for **p-PaF** and **p-PaF-OH**, respectively. When the obtained values are substituted to eq 4, the reorganization energy of the charge recombination,  $\lambda_{\text{ig}}$ , is calculated to be 1.05 eV. The value of the reorganization energy is considerably larger than the values reported previously for the chlorin–fullerene (0.484 eV<sup>20</sup>) and porphyrin–fullerene (0.66 eV<sup>38</sup>) systems but is relatively close to the value determined for porphyrin–quinone dyad (1.12 eV<sup>39</sup>).

The electronic coupling of the charge recombination,  $V_{\text{ig}}$ , can be calculated from eq 2 using the value of the reorganization energy obtained above and is 0.0019 eV (15  $\text{cm}^{-1}$ ). This is smaller than the value reported for compact porphyrin–fullerene systems,  $V = 140\text{--}270 \text{ cm}^{-1}$ ,<sup>7–9</sup> but larger than the values reported previously for chlorin–fullerene<sup>20</sup> ( $V = 6.93 \text{ cm}^{-1}$ ) and porphyrin–fullerene<sup>38</sup> ( $V = 3.9 \text{ cm}^{-1}$ ) dyads containing longer bridges between the two moieties.

The reorganization energy and the electronic coupling can be calculated for the partial charge-transfer reaction from the exciplex to the CCS state,  $(\text{PC})^* \rightarrow \text{P}^+\text{C}^-$ , in the same manner as described above for the transition from the CCS state to the ground state. The values of the reorganization energy and the electronic coupling are  $\lambda_{\text{xi}} = 0.38 \text{ eV}$  and  $V_{\text{xi}} = 0.0028 \text{ eV}$  (22  $\text{cm}^{-1}$ ), respectively.

**Degree of Charge Shift in the Exciplex and the Complete Charge-Transfer Distance.** On the basis of the reorganization energies of the reactions, it is possible to estimate the degree of the charge shift in the exciplex state. The solvent reorganization energy,  $\lambda_{\text{s}}$ , scales quadratically with the amount of charge,  $\Delta z$ , transferred in a delocalized charge transfer (CT) complex<sup>40</sup>

$$\Delta z = \left(\frac{\lambda_{\text{s,xi}}}{\lambda_{\text{s,ig}}}\right)^{1/2} \quad (5)$$

Here,  $\lambda_{\text{s,ig}}$  is the reorganization energy of the complete charge-transfer reaction, i.e., a reaction from the CCS state to the ground state, and  $\lambda_{\text{s,xi}}$  is the reorganization energy of a partial charge-transfer reaction from the exciplex to the CCS state.

The total nuclear reorganization energy is<sup>37</sup>  $\lambda = \lambda_{\text{s}} + \lambda_{\text{i}}$ , where  $\lambda_{\text{s}}$  is the solvent reorganization energy and  $\lambda_{\text{i}}$  is the internal reorganization energy. The internal reorganization energy of the  $(\text{PC})^* \rightarrow \text{PC}$  transition of several porphyrin–fullerene systems was found to be 0.03–0.13 eV.<sup>7–9,31</sup> The total reorganization energies of reactions  $(\text{PC})^* \rightarrow \text{P}^+\text{C}^-$  and  $\text{P}^+\text{C}^- \rightarrow \text{PC}$  are  $\lambda_{\text{xi}} = 0.38 \text{ eV}$  and  $\lambda_{\text{ig}} = 1.05 \text{ eV}$ , respectively. The values of total

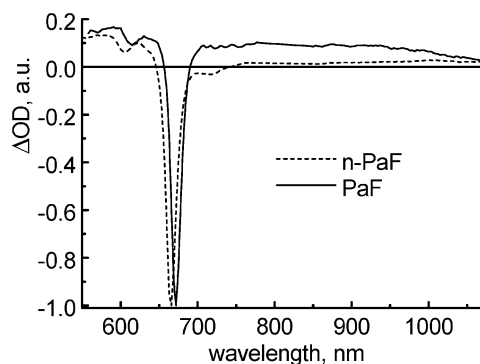


**Figure 10.** Comparison of the transient spectra at  $t = 0$  for **n-PaF** (dashed line) and **PaF** (solid line) in toluene.

reorganization energy are considerably larger than the values obtained earlier for the internal reorganization energy of quite similar systems. Therefore, in further discussion, it is assumed that  $\lambda_{\text{s}} \approx \lambda$ . When the values of the reorganization energies,  $\lambda_{\text{xi}}$  and  $\lambda_{\text{ig}}$ , are substituted to eq 5, the partial CT of  $(\text{PC})^* \rightarrow \text{P}^+\text{C}^-$  is  $\Delta z_{\text{xi}} = 0.6$ . Thus, the amount of charge transferred in the reaction  $\text{P}^{15}\text{C} \rightarrow (\text{PC})^*$  is  $\Delta z_{\text{px}} = 1 - \Delta z_{\text{xi}} = 0.4$ .

The distance of the complete charge separation can be estimated based on the dielectric continuum model of the solvent. The solvent reorganization energy is<sup>37</sup>

$$\lambda_{\text{s}} = \frac{q^2}{4\pi\epsilon_0} \left( \frac{1}{2r_{\text{D}}} + \frac{1}{2r_{\text{A}}} - \frac{1}{r_{\text{DA}}} \right) \left( \frac{1}{\epsilon_{\text{opt}}} - \frac{1}{\epsilon} \right) \quad (6)$$

where  $r_{\text{D}}$  and  $r_{\text{A}}$  are the radii of the donor and acceptor, respectively. For benzonitrile,  $\epsilon_{\text{opt}} = n^2 = 1.528^2 = 2.3348$  ( $n$  is the refractive index of the solvent) and  $\epsilon = 26$ . If  $r_{\text{D}} = 0.35 \text{ nm}$ ,  $r_{\text{A}} = 0.3 \text{ nm}$ , and  $\lambda_{\text{s}} \approx \lambda_{\text{ig}} = 1.05 \text{ eV}$ , eq 6 gives  $r_{\text{DA}} \approx 1 \text{ nm}$  for the CT distance, which is a reasonable value based on the molecular structure of the dyad.

**Comparison of the New Dyads with PaF and PbF.** The ET properties of the dyads, **n-PaF**, **n-PbF**, **p-PaF**, **p-PaF-OH**, and **p-PbF-OH**, differ considerably from the ET properties of earlier studied phytychlorin–fullerene dyads, **PaF** and **PbF**, even though the observed intermediate states are the same.<sup>15,16</sup> Structurally, the important difference between the new dyads and the dyads studied earlier is the bridge between the phytychlorin and fullerene moieties. The effect of the bridge alone can be observed by comparing **PaF** and **PbF** with **n-PaF** and **n-PbF**. **PaF** and **PbF** have only two single bonds separating the fullerene from the phytychlorin moiety, whereas the moieties in **n-PaF** and **n-PbF** are separated by four bonds.

For **PaF** and **PbF**, about half of the excited molecules form the exciplex directly from the  $\text{P}^{25}\text{C}$  state.<sup>15,16</sup> The process is not time-resolved ( $k > 5 \times 10^{12} \text{ s}^{-1}$ ) but is evident as seen in Figure 10, where the spectra at time delay  $t = 0$  are presented for **PaF** and **n-PaF** in toluene. **PaF** has a broad absorption between 700 and 1050 nm immediately after excitation, whereas **n-PaF** shows only a very weak absorption in that wavelength region. For any of the new dyads, the exciplex is not formed directly from the  $\text{P}^{25}\text{C}$  state likely because of the longer distance and, thus, lower electronic coupling between the phytychlorin and fullerene moieties.

A very efficient energy transfer from phytychlorin to fullerene was observed for **PaF** and **PbF** both in benzonitrile and in toluene ( $k_{\text{pc}} \approx 2 \times 10^{12} \text{ s}^{-1}$ ). For **n-PaF** and **n-PbF**, a transition takes place from the exciplex to first excited singlet state of fullerene and it is observed only in toluene and the rate constant is  $k_{\text{xc}} < 1 \times 10^{11} \text{ s}^{-1}$ . For **PaF** and **PbF**, the  $\text{PC}^{15}$  state decays



to the exciplex indicating that the exciplex energy is lower than the energy of PC<sup>15</sup>. For the present dyads, the situation is the opposite. The higher exciplex energies of **n-PaF** and **n-PbF** relative to **PaF** and **PbF** are due to the weaker interactions of the phytychlorin and fullerene moieties resulting from the longer bridge between the moieties.

For **PaF** and **PbF** in toluene, the lifetime of the exciplex is more than a nanosecond and a weak exciplex emission was observed.<sup>15,16</sup> Because of the lower electronic coupling of the donor and the acceptor of **n-PaF** and **n-PbF**, even weaker exciplex emission is expected because the yield is proportional to the square of the electronic coupling element.<sup>41,42</sup> In addition, the lifetime of the exciplex of **n-PaF** and **n-PbF** in toluene is reduced at least 40 times relative to **PaF** and **PbF**. On the basis of the relative energy of the exciplex state, the exciplex emissions of **n-PaF** and **n-PbF** would be expected around 700 nm, where also the phytychlorin moiety emits. Because of the low emission yield of the exciplex and the overlap of the exciplex emission band with the band of the phytychlorin moiety, it is not surprising that no experimental evidence of exciplex emission is observed for **n-PaF** and **n-PbF** or other new dyads.

Perhaps the most pronounced difference between the dyads studied in the present work and **PaF** and **PbF** is the formation efficiency of the CCS state. The new dyads, which are characterized by a longer donor–acceptor separation distance, form the CCS states even in nonpolar toluene with the quantum yields as high as 0.3–0.8, whereas the exciplexes of **PaF** and **PbF** relax directly to the ground states. In benzonitrile, the exciplex of **PbF** relaxes to the ground state without forming a CCS state.<sup>16</sup> By the cyclic voltammetry, the cation and anion radicals of **PbF** can be produced in benzonitrile, and the energy of the CCS state is 1.43 eV. The energy difference between the exciplex and the CCS state appears to be too low for the CCS formation for **PbF** even in polar benzonitrile, whereas **PaF** forms the CCS state with a rate constant of  $5 \times 10^{10} \text{ s}^{-1}$  and the quantum yield is estimated to be around 0.5.<sup>15</sup> The quantum yields of the CCS formations of the new dyads in benzonitrile are close to unity, and the rate constants are higher:  $7\text{--}25 \times 10^{10} \text{ s}^{-1}$ .

## Conclusions

The objective of the work was to design and synthesize a phytychlorin–fullerene dyad capable of photoinduced electron-transfer resulting into efficient formation of a complete-charge-separated (CCS) state even in nonpolar environment. Indeed, the new dyads (**n-PaF**, **n-PbF**, **p-PaF**, **p-PaF–OH**, and **p-PbF–OH**) form the CCS states in nonpolar toluene with the quantum yields of 0.3–0.8 controlled by the minor differences in the dyad structures. In contrast to the previously studied phytychlorin–fullerene dyads (**PaF** and **PbF**), the energies of the intramolecular exciplex states preceding the CCS states are increased due to a longer bridge between the phytychlorin and fullerene moieties. Because of the higher energy gap between the exciplex and the CCS state, the CCS state is formed more efficiently in the new dyads both in polar and nonpolar solvents. The results show that the most compact structure of the donor–acceptor pair may not be optimal from the point of complete charge separation. When the keto group is changed to the hydroxyl group at the position 13<sup>1</sup> of the phytychlorin macrocycle, the energy of the CCS state is decreased by about 0.19 eV and the quantum yield of the CCS state in nonpolar toluene is increased from 0.4 to 0.8.

## Experimental Section

The studied compounds are presented in Figure 1. The synthesis and NMR characterization of the **p-PaF** and **p-PbF–OH** dyads are reported earlier.<sup>19</sup> For the **n-PaF**, **n-PbF**, and **p-PaF–OH** dyads, the synthesis and characterization is described in SI.

Absorption spectra of the compounds were recorded on a Shimadzu UV-2501PC spectrophotometer. Fluorescence spectra were measured using a Fluorolog-3 fluorimeter (SPEX Inc.) and were corrected to the instrument wavelength sensitivity. The time-resolved fluorescence up-conversion and pump–probe systems and the data analysis procedures used in the experiments have been described in detail earlier.<sup>15</sup> In short, the samples were placed in a 1 mm thick rotating cuvette and excited by the second harmonic of the Ti:sapphire pulsed laser system at 400–420 nm to the second excited singlet state of the phytychlorin moiety, P<sup>2</sup>S<sub>C</sub>. The time resolution was approximately 150 fs for both instruments. The emission decays measured with fluorescence up-conversion were fitted to a sum of exponentials and provided the lifetimes of phytychlorin singlet state in different dyads. The time-resolved transient-absorption spectra were measured for all of the dyads in two wavelength regions (550–770 nm and 850–1070 nm). Typically, 50–60 spectra at different time delays were recorded. The results were combined and fitted globally to decay-associated spectra (DAS), which can be used to reconstruct the sample transient absorption with compensated probe pulse dispersion. The differential transient absorbance at wavelength  $\lambda$  and time  $t$  is given by  $\Delta A(\lambda, t) = \sum a_i(\lambda) \exp(-t/\tau_i)$  where  $a_i(\lambda)$  and  $\tau_i$  are the amplitudes and lifetimes of the components in the DAS. Because the time range of the instrument was 1 ns, the fitted lifetimes longer than that are inaccurate and can be treated as tentative values only.

The cyclic voltammetry experiments were performed in a three-electrode one-compartment cell connected to a BAS MF-9093 voltammetric analyzer. The working electrode consisted of a 0.5 mm in diameter platinum wire sealed in glass. The working electrode was polished with 0.3 and 0.05  $\mu\text{m}$  Al<sub>2</sub>O<sub>3</sub> before measurements. A platinum wire was used as the counter electrode and a Ag/AgCl electrode as reference electrode (Innovative Instruments, Inc.). All potentials are referred to this electrode and given as  $E_{1/2}$  values. The electrochemical measurements were performed at 23 °C in dry benzonitrile (BN, Acros) containing 0.1 M tetrabutylammonium hexafluorophosphate (TBAPF<sub>6</sub>, Fluka) as the electrolyte salt and 0.2–4 mM solutions of the phytychlorin–fullerene conjugates. TBAPF<sub>6</sub> was dried at 80 °C for 1 h under vacuum conditions before use. All solutions were purged with dry nitrogen several minutes before the electrochemical measurements. The potential cycling was performed between 0 and +1.2 V and between 0 and –2.0 V vs Ag/AgCl. The scan rate used was in the range of 50–400 mV/s.

**Acknowledgment.** The work was supported by the Academy of Finland and the National Technology Agency of Finland. V.V. thanks the Graduate School of Natural Sciences at Tampere University of Technology for funding.

**Supporting Information Available:** Synthesis of the compounds. Derivation of intrinsic rate constants and spectra of intermediate states. This material is available free of charge via the Internet at <http://pubs.acs.org>.

## References and Notes

- (1) Imahori, H.; Hagiwara, K.; Aoki, M.; Akiyama, T.; Taniguchi, S.; Okada, T.; Shirakawa, M.; Sakata, Y. *J. Am. Chem. Soc.* **1996**, *118*, 11771.
- (2) Kuciauskas, D.; Lin, S.; Seely, G. R.; Moore, A. L.; Moore, T. A.; Gust, D.; Drovetskaya, T.; Reed, C. A.; Boyd, P. D. W. *J. Phys. Chem.* **1996**, *100*, 15926.
- (3) Imahori, H.; Sakata, Y. *Eur. J. Org. Chem.* **1999**, 2445.
- (4) Schuster, D. I.; Cheng, P.; Wilson, S. R.; Prokhorenko, V.; Katterle, M.; Holzwarth, A. R.; Braslavsky, S. E.; Klihm, G.; Williams, R. M.; Luo, C. *J. Am. Chem. Soc.* **1999**, *121*, 11599.
- (5) Schuster, D. I. *Carbon* **2000**, *38*, 1607.
- (6) Armaroli, N.; Marconi, G.; Echegoyen, L.; Bourgeois, J.-P.; Diederich, F. *Chem. Eur. J.* **2000**, *6*, 1629.
- (7) Tkachenko, N. V.; Guenther, C.; Imahori, H.; Tamaki, K.; Sakata, Y.; Fukuzumi, S.; Lemmetyinen, H. *Chem. Phys. Lett.* **2000**, 326, 344.
- (8) Imahori, H.; Tkachenko, N. V.; Vehmanen, V.; Tamaki, K.; Lemmetyinen, H.; Sakata, Y.; Fukuzumi, S. *J. Phys. Chem. A* **2001**, *105*, 1750.
- (9) Vehmanen, V.; Tkachenko, N. V.; Imahori, H.; Fukuzumi, S.; Lemmetyinen, H. *Spectrochim. Acta A* **2001**, *57*, 2229.
- (10) Imahori, H.; Ozawa, S.; Ushida, K.; Takahashi, M.; Azuma, T.; Ajavakom, A.; Akiyama, T.; Hasegawa, M.; Taniguchi, S.; Okada, T.; Sakata, Y. *Bull. Chem. Soc. Jpn.* **1999**, *72*, 485.
- (11) Imahori, H.; Norieda, H.; Yamada, H.; Nishimura, Y.; Yamazaki, I.; Sakata, Y.; Fukuzumi, S. *J. Am. Chem. Soc.* **2001**, *123*, 100.
- (12) Kuciauskas, D.; Liddell, P. A.; Lin, S.; Johnson, T. E.; Weghorn, S. J.; Lindsey, J. S.; Moore, A. L.; Moore, T. A.; Gust, D. *J. Am. Chem. Soc.* **1999**, *121*, 8604.
- (13) Prokhorenko, V. I.; Holzwarth, A. R.; Müller, M. G.; Schaffner, K.; Miyatake, T.; Tamiaki, H. *J. Phys. Chem. B* **2002**, *106*, 5761.
- (14) Helaja, J.; Tauber, A. Y.; Abel, Y.; Tkachenko, N. V.; Lemmetyinen, H.; Kilpeläinen, I.; Hynninen, P., H. *J. Chem. Soc., Perkin Trans. 1* **1999**, 2403.
- (15) Tkachenko, N. V.; Rantala, L.; Tauber, A. Y.; Helaja, J.; Hynninen, P. H.; Lemmetyinen, H. *J. Am. Chem. Soc.* **1999**, *121*, 9378.
- (16) Vehmanen, V.; Tkachenko, N. V.; Tauber, A. Y.; Hynninen, P. H.; Lemmetyinen, H. *Chem. Phys. Lett.* **2001**, *345*, 213.
- (17) Tkachenko, N. T.; Vuorimaa, E.; Kesti, T.; Alekseev, A. S.; Tauber, A. Y.; Hynninen, P. H.; Lemmetyinen, H. *J. Phys. Chem. B* **2000**, *104*, 6371.
- (18) Alekseev, A. S.; Tkachenko, N. V.; Tauber, A. Y.; Hynninen, P. H.; Osterbacka, R.; Stubb, H.; Lemmetyinen, H. *Chem. Phys.* **2002**, *275*, 243.
- (19) Efimov, A.; Tkatchenko, N. V.; Vainiotalo, P.; Lemmetyinen, H. *J. Porphyrins Phthalocyanines* **2001**, *5*, 835.
- (20) Fukuzumi, S.; Ohkubo, K.; Imahori, H.; Shao, J.; Ou, Z.; Zheng, G.; Chen, Y.; Pandey, R. K.; Fujitsuka, M.; Ito, O.; Kadish, K. M. *J. Am. Chem. Soc.* **2001**, *123*, 10676.
- (21) Holzwarth, A. R.; Katterle, M.; Müller, M. G.; Ma, Y. Z.; Prokhorenko, V. *Pure Appl. Chem.* **2001**, *73*, 469.
- (22) Zheng, G.; Dougherty, T. J.; Pandey, R. K. *Chem. Commun.* **1999**, 2469.
- (23) Kutzki, O.; Walter, A.; Montforts, F.-P. *Helv. Chim. Acta* **2000**, *83*, 2231.
- (24) Montforts, F.-P.; Kutzki, O. *Angew. Chem., Int. Ed.* **2000**, *39*, 599.
- (25) Lee, J.-C.; Kim, T.-Y.; Kang, S. H.; Shim, Y. K. *Bull. Korean Chem. Soc.* **2001**, *22*, 257.
- (26) Kureishi, Y.; Tamiaki, H.; Shiraiishi, H.; Maruyama, K. *Bioelectrochem. Bioenerg.* **1999**, *48*, 95.
- (27) Kato, T.; Kodama, T.; Shida, T.; Nakagawa, T.; Matsui, Y.; Suzuki, S.; Shiromaru, H.; Yamauchi, K.; Achiba, Y. *Chem. Phys. Lett.* **1991**, *180*, 446.
- (28) Greaney, M. A.; Gorum, S. M. *J. Phys. Chem.* **1991**, *95*, 7142.
- (29) Sun, Y.; Drovetskaya, T.; Bolskar, R. D.; Bau, R.; Boyd, P. D. W.; Reed, C. A. *J. Org. Chem.* **1997**, *62*, 3642.
- (30) Fukuzumi, S.; Nakanishi, I.; Maruta, J.; Yorisue, T.; Suenobu, T.; Itoh, S.; Arakawa, R.; Kadish, K. M. *J. Am. Chem. Soc.* **1998**, *120*, 6673.
- (31) Kesti, T. J.; Tkachenko, N. V.; Vehmanen, V.; Yamada, H.; Imahori, H.; Fukuzumi, S.; Lemmetyinen, H. *J. Am. Chem. Soc.* **2002**, *124*, 8067.
- (32) Sension, R. J.; Philips, C. M.; Szarka, A. Z.; Romanow, W. J.; McGhie, A. R.; McCauley, J. P., Jr.; Smith, A. B., III.; Hochstrasser, R. M. *J. Phys. Chem.* **1991**, *95*, 6075.
- (33) Ebbesen, T. W.; Tanigaki, K.; Kuroshima, S. *Chem. Phys. Lett.* **1991**, *181*, 501.
- (34) Palit, D. K.; Sapre, A. V.; Mittal, J. P.; Rao, C. N. R. *Chem. Phys. Lett.* **1992**, *195*, 1.
- (35) Fujitsuka, M.; Ito, O.; Yamashiro, T.; Aso, Y.; Otsubo, T. *J. Phys. Chem. A* **2000**, *104*, 4876.
- (36) Imahori, H.; El-Khouly, M. E.; Fujitsuka, M.; Ito, O.; Sakata, Y.; Fukuzumi, S. *J. Phys. Chem. A* **2001**, *105*, 325.
- (37) Wasielewski, M. R. *Chem. Rev.* **1992**, *92*, 435.
- (38) Imahori, H.; Tamaki, K.; Guldi, D. M.; Luo, C.; Fujitsuka, M.; Ito, O.; Sakata, Y.; Fukuzumi, S. *J. Am. Chem. Soc.* **2001**, *123*, 2607.
- (39) Tsue, H.; Imahori, H.; Kaneda, T.; Tanaka, Y.; Okada, T.; Tamaki, K.; Sakata, Y. *J. Am. Chem. Soc.* **2000**, *122*, 2279.
- (40) Matyushov, D. V.; Voth, G. A. *J. Phys. Chem. A* **2000**, *104*, 6470.
- (41) Marcus, R. A. *J. Phys. Chem.* **1989**, *93*, 3078.
- (42) Gould, I. R.; Young, R. H.; Moody, R. E.; Farid, S. *J. Phys. Chem.* **1991**, *95*, 2068.